

This material may be protected by  
copyright law (Title 17 U.S. Code)

# Time Course of Pulmonary Response of Rats to Inhalation of Crystalline Silica: Histological Results and Biochemical Indices of Damage, Lipidosis, and Fibrosis

Dale W. Porter,<sup>1</sup> Dawn Ramsey,<sup>2</sup> Ann F. Hubbs,<sup>1</sup> Lori Battelli,<sup>1</sup> Jane Ma,<sup>1</sup> Mark Barger,<sup>1</sup>  
Douglas Landsittel,<sup>1</sup> Victor A. Robinson,<sup>1</sup> Jeff McLaurin,<sup>2</sup> Amir Khan,<sup>2</sup>  
William Jones,<sup>3</sup> Alexander Teass,<sup>2</sup> & Vincent Castranova<sup>1</sup>

---

Previous studies have determined that  $\alpha$ -quartz (crystalline silica) can cause pulmonary inflammation, damage, and fibrosis. However, the temporal relationship between silica inhalation and pulmonary inflammation, damage, and fibrosis has not been fully examined. To address this gap in our knowledge of silica-induced pulmonary fibrosis, a chronic inhalation study using rats was designed. Specifically, rats were exposed to a silica aerosol (15 mg/m<sup>3</sup> silica, 6 h/d, 5d/wk, 116 d), and measurements of pulmonary inflammation, damage, and fibrosis were monitored throughout the study. We report (1) data demonstrating that the silica aerosol generation and exposure system produced a consistent silica aerosol of respirable size particles; (2) the time course of silica deposition in the lung; (3) calculations that demonstrate that the rats were not in pulmonary overload; (4) histopathological data demonstrating time-dependent enhancement of silica-induced alveolitis, epithelial hypertrophy and hyperplasia, alveolar lipoproteinosis, and pulmonary fibrosis in the absence of overload; and (5) biochemical data documenting the development of lipidosis, lung damage, and fibrosis.

---

**KEYWORDS:**  $\alpha$ -quartz, silica, inhalation exposure, silicosis, pulmonary fibrosis, alveolar lipoproteinosis

## Introduction

Crystalline silica ( $\alpha$ -quartz) aerosols are produced in a number of industrial processes and occupations, resulting in silica inhalation by exposed workers. Silica inhalation in humans has been linked to a disease commonly referred to as *silicosis* and is gener-

ally characterized by a severe decline in respiratory function and premature death.<sup>1</sup> In 1986, the National Institute for Occupational Safety and Health (NIOSH) estimated that 2.3 million workers were exposed to silica,<sup>2</sup> and approximately 1500 cases of silicosis are diagnosed every year in the United States.<sup>3</sup> This may represent an underestimate of the

---

National Institute for Occupational Safety and Health:  
<sup>1</sup>Health Effects Laboratory Division, Morgantown, WV;  
<sup>2</sup>Division of Applied Research and Technology, Cincinnati, OH; <sup>3</sup>Division of Respiratory Disease Studies, Morgantown, WV. Correspondence: Vincent Castranova,

Ph.D., Branch Chief, Pathology and Physiology Research Branch, Health Effects Laboratory Division, National Institutes for Occupational Safety and Health, 1095 Willowdale Road, M/S 2015, Morgantown, WV 26505; V.Castranova@cdc.gov.

true incidence of silicosis, because it is suspected that many silicosis cases are unreported.

Previous inhalation studies have used several different exposure study designs to examine the mechanisms of silica toxicity and pathogenesis. One approach has been to conduct acute exposures to silica aerosol concentrations ranging from 11.2 mg/m<sup>3</sup> for 8 days<sup>4</sup> and 44.5 mg/m<sup>3</sup> for 8 days,<sup>5</sup> to 50 mg/m<sup>3</sup> silica aerosol for 5 days.<sup>6</sup> In these studies, silica-induced mechanisms of pulmonary inflammation and pathogenesis were examined at various times after exposure. Another approach has been to conduct subchronic exposures to silica aerosol concentrations of 0.1–10 mg/m<sup>3</sup> silica for 4 weeks,<sup>7</sup> 3 mg/m<sup>3</sup> for 13 weeks,<sup>8</sup> and 2 mg/m<sup>3</sup> for up to 6 months,<sup>9</sup> but only one or three exposure times were examined in these studies. A 2-year chronic inhalation study conducted to assess toner carcinogenicity included a 1 mg/m<sup>3</sup> silica exposure, but measurements of pulmonary inflammation and damage were limited to 15, 21, and 24 months of exposure.<sup>10</sup>

Although providing substantial mechanistic information, these silica inhalation studies did not establish the detailed temporal relationships among silica inhalation, pulmonary inflammation and damage, and the development of pulmonary fibrosis. Indeed, a recent workshop on poorly soluble particles concluded that a significant gap in our knowledge exists concerning the temporal sequence of molecular, cellular, and histopathological changes that occur after exposure to poorly soluble particles, such as silica.<sup>11</sup>

Therefore, we initiated a study in which the comprehensive goal was to investigate in detail the temporal relationship between silica inhalation, lung particle burden, and the initiation and progression of adverse pulmonary responses in the rat model. In the first in a series of articles from this study, we report (1) data demonstrating that the silica aerosol generation and exposure system produced a consistent silica aerosol of respirable size particles; (2) the time course of silica deposition in the lung; (3) calculations demonstrating that the rats were not in pulmonary overload; (4) histopathological data demonstrating time-dependent enhancement of silica-induced alveolitis, epithelial hypertrophy and hyperplasia, alveolar lipoproteinosis, and pulmonary fibrosis in the absence of overload; and (5) biochemical data documenting the development of lipodosis, lung damage, and fibrosis.

## Materials and Methods

### *Silica Chemical Analyses*

The silica used in this study was Min-U-Sil 5 (US Silica, Berkeley Springs, WV, USA). Bulk silica was examined by proton-induced X-ray emission (PIXE) spectrometry for inorganic contaminants and for desorbable organic carbon compounds by gas chromatography mass spectrometry. Aerosolized silica samples were examined for trace inorganic elements by PIXE spectrometry and for elemental and organic carbon using a thermal-optical analyzer.

### *Exposure of Rats to Silica Aerosol*

Specific pathogen-free male Fischer 344 rats (strain CDF, 75–100 g) were purchased from Charles River (Raleigh, NC, USA) and housed in an AAALAC-approved animal facility using individual cages in two 5 m<sup>3</sup> Hinners-type inhalation chambers. All animal protocols were approved by the Animal Care and Use Committee of the National Institute for Occupational Safety and Health. The rats were acclimated to the chambers for 1 week prior to the start of the study. One chamber was used for filtered-air exposures (control) and the other for 15 mg/m<sup>3</sup> silica exposures. Exposures were conducted 6 hours per day, 5 days per week, for a total of 116 exposure days. Water was available ad libitum, and food was available at all times except during exposures. The rats were on a 12-hour light–dark schedule and were exposed during the dark cycle to coincide with their most active period. Each chamber had 10–12 air changes per hour and an inside pressure of 25 Pa less than the ambient laboratory pressure. The air was rough filtered, heated or chilled to approximately 16 °C, and then reheated as necessary to maintain a temperature between 22.2 and 25.6 °C within the chambers. The air then passed through a high-efficiency particle filter, a charcoal bed, and a medium-efficiency filter before humidification with a steam humidifier. Target levels for temperature (22.2–25.6 °C), humidity (40–70%), and ammonia (≤5 ppm) were based on recommendations of the National Toxicology Program<sup>12</sup> and were monitored continuously with a computer data acquisition system. The in-

halation chamber temperature, relative humidity, and ammonia showed no significant deviations from the target levels during the study.

The silica aerosol generation system consisted of a twin screw feeder and funnel that deposited silica onto a rotating plate. Static charge on the rotating plate was dissipated with 3 polonium-210 ionizing units positioned above the rotating plate. An aspirator positioned over the rotating plate aerosolized the silica using breathing grade compressed air, which had been filtered through an active carbon bed. The aerosol stream then passed through a cyclone and into the main air-supply duct to the chamber. Mixing of the streams was effected by an orifice plate 3 cm upstream and a baffle 17 cm downstream of the point of entry of the aerosol stream into the duct. The charge on the dust was neutralized by a pulsed air ionizer located in the main duct upstream of the orifice plate.

Silica aerosol concentration in the chamber was monitored continuously with a RAS-2 particle sensor and gravimetrically using polyvinylchloride membrane filters (37 mm, 5  $\mu$ m pore size) changed at 1 hour intervals throughout the study. Particle size was measured with an Andersen 8-stage cascade impactor on 8 predetermined days of exposure. Simultaneously, polycarbonate filter (25 mm, 0.1  $\mu$ m pore size) samples were collected for scanning electron microscopic examination of the aerosol.

### ***Bronchoalveolar Lavage***

Rats were euthanized with an i.p. injection of  $\geq 100$  mg sodium pentobarbital/kg body weight after 5, 10, 16, 20, 30, 41, 79, and 116 days exposure. A tracheal cannula was inserted and bronchoalveolar lavage (BAL) was conducted through the cannula using ice cold  $\text{Ca}^{2+}$  and  $\text{Mg}^{2+}$  free phosphate-buffered saline (PBS) with 5.5 mM D-glucose added. The first BAL of 6 mL was kept separate from the subsequent lavages with 8 mL of PBS, until a total of 80 mL was collected. BAL cells were isolated by centrifugation ( $650 \times g$ , 10 min,  $4^\circ\text{C}$ ). The acellular supernatant from the first BAL (BAL fluid) was decanted and transferred to plastic tubes for later analyses or storage at  $-30^\circ\text{C}$ . The acellular supernatants from the other lavages were decanted and discarded. BAL cells from the first and subsequent lavages for each rat

were resuspended in a HEPES buffer (10 mM *N*-[2-hydroxyethyl]piperazine-*N'*-[2-ethanesulfonic acid], 145 mM NaCl, 5 mM KCl, 1 mM  $\text{CaCl}_2$ , 5.5 mM D-glucose, pH 7.4) and combined. The BAL cells were centrifuged ( $650 \times g$ , 10 min,  $4^\circ\text{C}$ ) and the supernatants decanted and discarded. The BAL cell pellet was resuspended in the HEPES buffer and placed on ice for later use.

### ***BAL Fluid Total Protein***

BAL fluid total protein concentration was determined colorimetrically at 540 nm using the Biuret reaction.

### ***BAL Fluid Phospholipid***

Phospholipids were measured as the phosphorus present in lipid extracts of BAL fluid. Lipid was extracted from BAL fluid by mixing a 0.5 mL BAL fluid sample with 10 mL  $\text{CHCl}_3$ :MeOH (2:1, v/v). After 1.5 hours' incubation at room temperature, 2 mL ice-cold 0.1 M KCl was added, and the samples were manually mixed by inversion for 2 minutes. The samples were then centrifuged at 2500 rpm (IEC HN-S Centrifuge) for 5 minutes. After centrifugation, the top layer was removed by aspiration, and the bottom layer was washed three times by addition and aspiration of  $\text{CHCl}_3$ :MeOH: $\text{H}_2\text{O}$  (3:48:47, v/v/v) with a Pasteur pipet, then dried under nitrogen gas at  $50^\circ\text{C}$ . After the samples were dried, 0.5 mL each of water and 10 N  $\text{H}_2\text{SO}_4$  was added. The samples were heated overnight at  $150$ – $160^\circ\text{C}$ , followed by addition of 100  $\mu\text{L}$  of 30%  $\text{H}_2\text{O}_2$  and heating at  $150$ – $160^\circ\text{C}$  for an additional 1.5 hours. The samples were allowed to cool to room temperature and inorganic phosphate determined colorimetrically at 830 nm by a modification of the Fiske Subbarow method.<sup>13</sup> Inorganic phosphate standards used for the standard curve were processed concurrently with the experimental samples. The phospholipid content of BAL fluid was calculated by multiplying the lipid phosphorous by 25.<sup>14</sup>

### ***Lung Silica Burden***

Rats were euthanized after 1, 5, 10, 20, 41, 79, and 116 days of exposure with an ip injection ( $\geq 100$

mg/kg body weight) of sodium pentobarbital. The lungs were removed, weighed, frozen in liquid nitrogen, and pulverized with a mortar and pestle. A sample of the pulverized lung sample was weighed and lyophilized. After lyophilization, the lung tissue was weighed and transferred into 50-mL Griffin-style teflon beakers. The samples were treated with 10 mL of concentrated  $\text{HNO}_3$  and 1 mL 70%  $\text{HClO}_4$ , covered, and refluxed overnight at 150 °C. The covers were removed the next day and the samples taken to perchloric fumes at the same temperature. An additional 5 mL of  $\text{HNO}_3$  was added, and the samples were taken to near dryness to remove the organic matrix. The residues were dissolved with 0.5 mL of hydrofluoric acid, quantitatively transferred to graduated centrifuge tubes, and diluted to 10.0 mL final volume. Samples were analyzed by inductively coupled plasma-atomic emission spectroscopy (ICP-AES) for silicon using matrix-matched standards for comparison. The determinations were made at 288.158, 251.432, and 252.411 nm. Three replicate aliquots of Min-U-Sil 5 were carried through the entire procedure in conjunction with the tissue samples. The average  $\text{SiO}_2$  recovery of these samples was 100.2% (range, 97.1–103.1).

### *Lung Hydroxyproline*

Rats were euthanized at 10, 20, 41, 79, and 116 days of exposure with an ip injection ( $\geq 100$  mg/kg body weight) of sodium pentobarbital. The lungs were removed en bloc, washed in ice-cold 0.9% (w/v) NaCl, blotted dry, and weighed. The lung tissue was then processed to determine hydroxyproline, as previously described.<sup>15,16</sup>

### *Lung Histopathology*

Rats were euthanized at 1, 5, 10, 20, 41, 79, and 116 days of exposure with an ip injection ( $\geq 100$  mg/kg body weight) of sodium pentobarbital, and the lungs were airway perfused by inflation with glutaraldehyde solution at 20 cm  $\text{H}_2\text{O}$  pressure. Subsequently, the lungs were embedded in paraffin, sectioned at a thickness of 5  $\mu\text{m}$ , and stained with hematoxylin and eosin and Masson's trichrome. Slides were examined by a board-certified veteri-

nary pathologist. Tissue alterations were scored for severity (0 = none, 1 = minimal, 2 = mild, 3 = moderate, 4 = severe) and distribution (0 = none, 1 = focal, 2 = locally extensive, 3 = multifocal, 4 = multifocal and severe, 5 = diffuse), as previously described.<sup>17</sup> The histopathology score was the sum of lesion severity and distribution scores.

### *Statistical Analyses*

The difference between air- and silica-exposed rats at each time point was tested using appropriate contrasts in the two-way analysis of variance model with interaction.<sup>18</sup> A log transformation of the response variable was used to satisfy assumptions of normality and constant variance. Because of its discrete nature, analyses of histopathological scores were limited to pair-wise rank-sum tests, which is the nonparametric version of the  $t$  test.<sup>19</sup> The comparisons made were between the air- and silica-exposed groups at each exposure time, and between adjacent exposure time points for silica-exposed rats. To characterize toxicity changes over time for all other responses, data were fit to a linear regression model that included any statistically significant polynomial terms, up to a cubic term. Predicted values and associated confidence intervals from the regression model<sup>20</sup> were used to identify significant differences between exposure times (i.e., time points with nonoverlapping confidence intervals) within the silica-exposed animals. This approach was preferable to doing pairwise tests of mean values, because the regression model fits a single curve to the dose-response relationship over the entire range of data.

## **Results**

### *Silica Chemical Analyses*

Bulk silica was examined by PIXE spectrometry and determined to be  $\geq 98.5\%$  pure quartz with low inorganic contamination ( $\leq 0.10\%$ ). Bulk silica was also analyzed for desorbable organic carbon compounds by gas chromatography mass spectrometry, and only trace levels were found. Aerosolized silica samples were examined for trace inorganic elements by PIXE spectrometry. Results indicate that the silica had only trace amounts of iron, calcium, titanium, and zinc (average total trace elements = 0.13%). Aerosolized sil-

**TABLE 1.** Gravimetric Determination of Silica Aerosol Concentration

Exposure days	Number of samples	Silica aerosol concentration (mg/m <sup>3</sup> ) <sup>a</sup>
1-5	30	15.5 ± 0.19
6-10	30	14.9 ± 0.40
11-16	35	15.3 ± 0.21
17-20	24	15.3 ± 0.32
21-30	60	15.3 ± 0.26
31-41	65	15.2 ± 0.23
42-79	228	15.3 ± 0.11
80-116	220	15.2 ± 0.10

<sup>a</sup> Values represent means ± SE.

ica samples were also analyzed for elemental and organic carbon using a thermal-optical analyzer. Total carbon averaged 0.10% of the silica aerosol.

#### *Exposure Chamber Environment*

The silica aerosol concentration was remarkably stable over the course of the 116-day exposure, with average weekly values ranging from 14.9 to 15.5 mg/m<sup>3</sup> (Table 1). The mass median aerodynamic diameter of the silica aerosol was consistently ≤2 μm (Table 2).

As an alternative means for evaluating the constancy of chamber conditions, scanning electron microscopic images of air samples collected within the exposure chamber were examined (Fig. 1). Images A and B are from samples collected on exposure days 32 and 98, respectively. These samples are matched in terms of sample time, flow rate, location, and magnification. The particle densities and size ranges on these images can thus be directly compared for a visual indication of how well these parameters were maintained over time. Images C and D are higher magnification images of particles iso-

**TABLE 2.** Silica Aerosol Particle Size Characterization

Exposure day	Mass median aerodynamic diameter (μm)	Geometric standard deviation
6	1.70	1.78
27	1.54	1.88
32	1.47	1.92
36	1.58	1.76
42	1.60	1.89
55	1.60	1.82
81	1.86	1.83
98	1.57	1.81

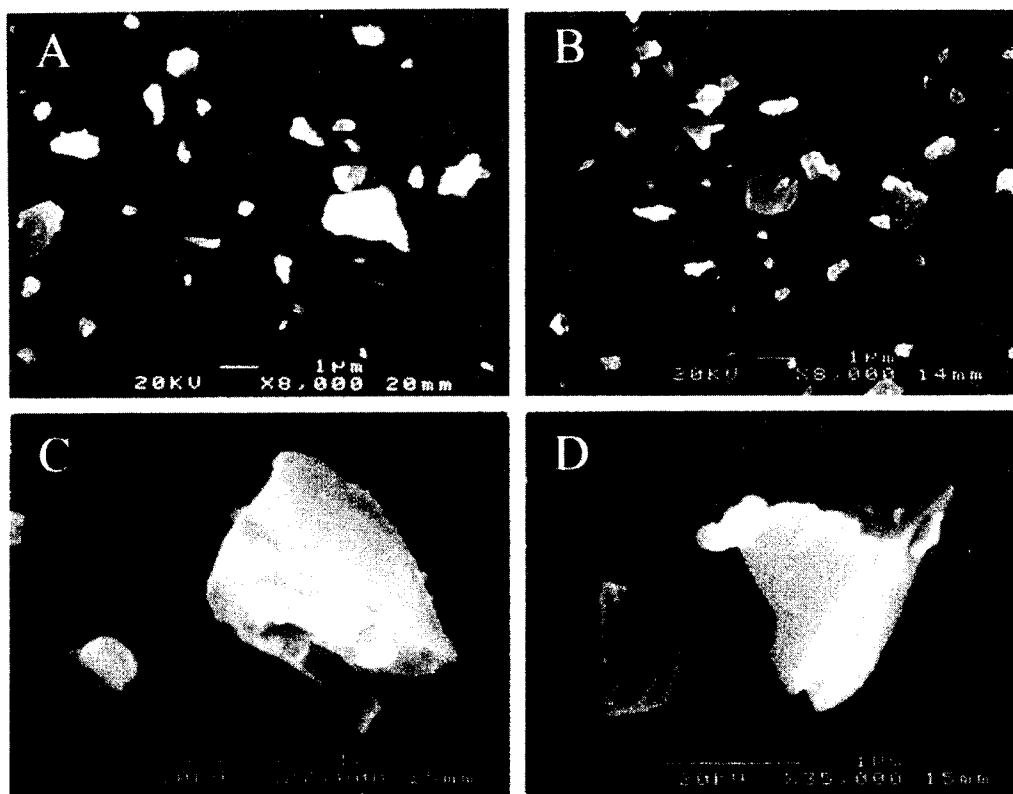


**FIGURE 1.** Scanning electron micrographs of air samples collected from the silica exposure chamber. (A) and (B): lower magnification of chamber air samples collected on exposure days 32 and 98, respectively. (C) and (D): higher magnification of chamber air samples collected on exposure day 42.

lated from a sample collected on day 42. Note the sharp, angular cleavage patterns characteristic of crystalline silica.

### *Body and Lung Weights*

Rat body and lung weights were monitored throughout the study. Small but significant differences in body weight between air- and silica-exposed rats were observed only at 79 and 116 days of exposure (Fig. 2). Silica-exposed rats had significantly higher lung weights versus control at all exposure times from 10 to 116 days of exposure (Fig. 3). Furthermore, for silica-exposed rats, lung weights at 10 and 20 days of exposure were significantly lower ( $p \leq 0.05$ ) than that determined at 41 days of exposure, which was

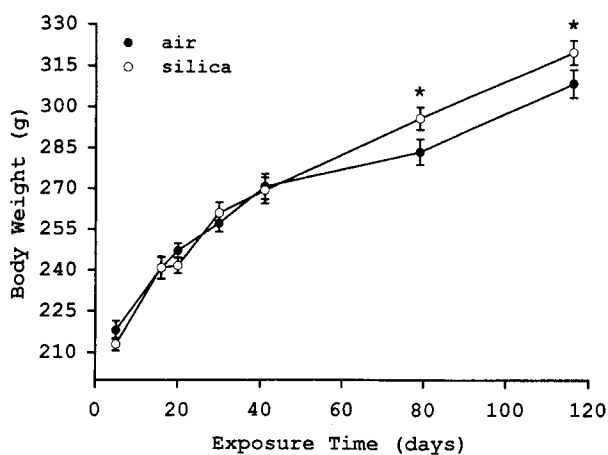


**FIGURE 2.** Rat body weights. Values represent means  $\pm$  SE ( $N = 6-31$ ). An asterisk indicates significant difference ( $p \leq 0.05$ ) between air-exposed control and silica-exposed rats at a given exposure time.

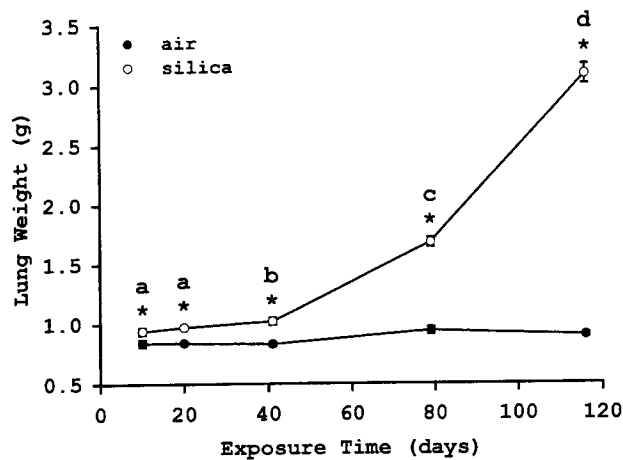


**FIGURE 3.** Rat lung weights. Values represent means  $\pm$  SE ( $N=6$ ). An asterisk indicates significant difference ( $p \leq 0.05$ ) between air-exposed control and silica-exposed rats at a given exposure time. For silica-exposed rats, exposure times with different letters are significantly different from each other ( $p \leq 0.05$ ).

followed by further significant increases ( $p \leq 0.05$ ) at 79 and 116 days of exposure (Fig. 3).

### Lung Silica Burden

Lung silica burden increased progressively, with statistically significant ( $p \leq 0.05$ ) increases in silica lung

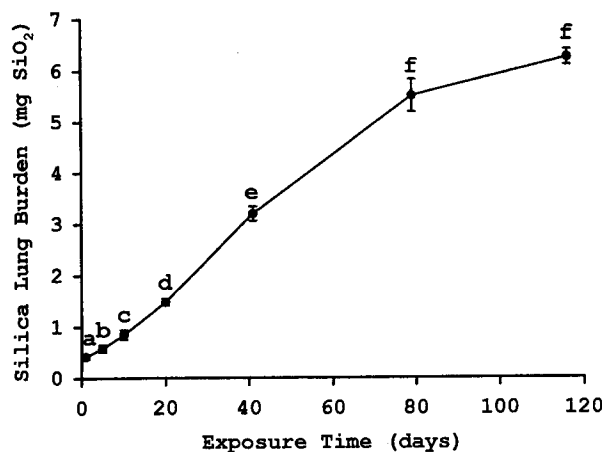


**FIGURE 4.** Silica lung burden. Values represent means  $\pm$  SE ( $N=6$ ). Exposure times with different letters are significantly different ( $p \leq 0.05$ ) from the immediately preceding exposure time.

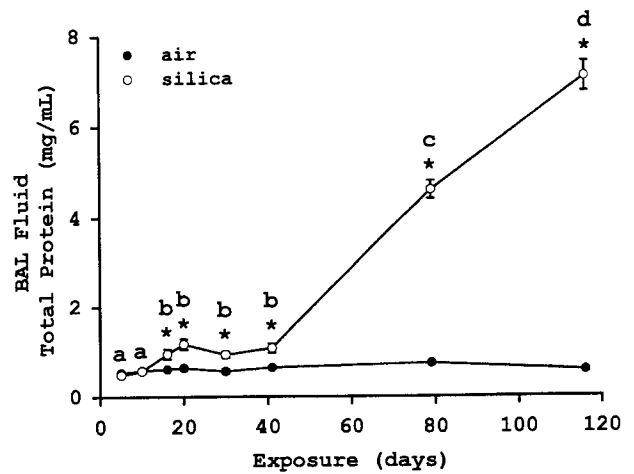


**FIGURE 5.** BAL fluid total protein concentration. Values represent means  $\pm$  SE ( $N=15$ ). An asterisk indicates significant difference ( $p \leq 0.05$ ) between air-exposed control and silica-exposed rats at a given exposure time. For silica-exposed rats, exposure times with different letters are significantly different from each other ( $p \leq 0.05$ ).

burden from the start of the silica exposure through 79 days of exposure (Fig. 4). However, between 79 and 116 days of exposure, the lung silica burden did not significantly differ ( $p \geq 0.05$ ).

### BAL Fluid Total Protein

In comparison to control rats, silica-exposed rats had significantly higher ( $p \leq 0.05$ ) levels of total protein in BAL fluid from 16 to 116 days of exposure (Fig. 5). Furthermore, acellular BAL total protein levels in silica-exposed rats significantly increased with continued exposure. Acellular BAL total protein at 5 and 10 days of exposure was significantly lower ( $p \leq 0.05$ ) than that determined between 16 and 41 days of exposure, which was followed by further significant increases ( $p \leq 0.05$ ) at 79 and 116 days of exposure.

### BAL Fluid Phospholipids

Silica-exposed rats had significantly higher ( $p \leq 0.05$ ) levels of phospholipids in BAL fluid at all exposure times compared with controls, except at 10 days of exposure (Fig. 6). Acellular BAL phospho-

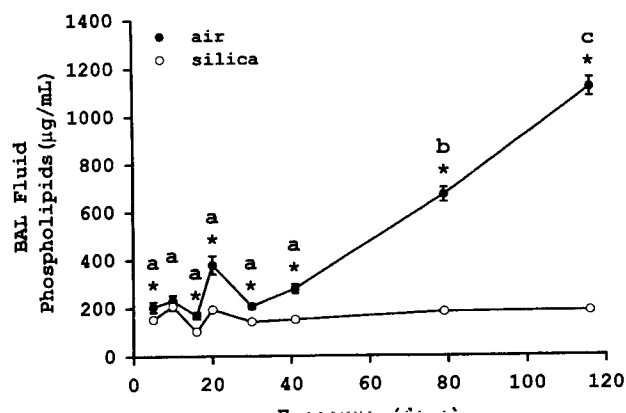


**FIGURE 6.** BAL fluid phospholipid concentration. Values represent means  $\pm$  SE ( $N=15$ ). An asterisk indicates significant difference ( $p \leq 0.05$ ) between air-exposed control and silica-exposed rats at a given exposure time. For silica-exposed rats, exposure times with different letters are significantly different from each other ( $p \leq 0.05$ ).

lipid levels in silica-exposed rats significantly increased with continued exposure. Acellular BAL phospholipid levels from 5 to 41 days of exposure averaged 63% lower ( $p \leq 0.05$ ) than that determined at 79 days of exposure, which was 40% lower ( $p \leq 0.05$ ) than at 116 days of exposure.

### Pulmonary Fibrosis

Pulmonary fibrosis was examined using two independent methods. A biochemically based assay used hydroxyproline as the marker of fibrosis. The hydroxyproline determinations indicate that the only statistically significant difference between air- and silica-exposed rat lung hydroxyproline levels was at 116 days of exposure (Table 3). Pulmonary fibrosis was also evaluated histologically using lung sections stained with Masson's trichrome (see Fig. 7 on page 11). Histological examination of air- and silica-exposed rat lungs showed that only silica-exposed lungs had developed fibrosis, and fibrosis was first observed at 79 days of exposure and was more severe at 116 days of exposure (Table 3).

### Pulmonary Histopathology

Alveolitis, alveolar epithelial hypertrophy and hyperplasia, and alveolar lipoproteinosis were evaluated after inhalation of silica throughout the exposure (Fig. 8). Histopathological alterations in control and silica-exposed rat lungs are summarized in Table 4. No histopathological alterations were observed at 1, 5, or 10 days of exposure. At 20 days' exposure, the pulmonary response was characterized by multifocal,

**TABLE 3.** Pulmonary Fibrosis

Exposure day	Lung hydroxyproline (mg/lung) <sup>a</sup>		Fibrosis histopathology scores <sup>b,c</sup>	
	Air	Silica	Air	Silica
1	N.D.	N.D.	N.D.	0.0 $\pm$ 0.0
5	N.D.	N.D.	N.D.	0.0 $\pm$ 0.0
10	1.73 $\pm$ 0.16	1.38 $\pm$ 0.13	0.0 $\pm$ 0.0	0.0 $\pm$ 0.0
20	0.92 $\pm$ 0.07	0.85 $\pm$ 0.09	0.0 $\pm$ 0.0	0.0 $\pm$ 0.0
41	0.67 $\pm$ 0.03	0.88 $\pm$ 0.07	0.0 $\pm$ 0.0	0.0 $\pm$ 0.0
79	2.04 $\pm$ 0.11	1.86 $\pm$ 0.29	0.0 $\pm$ 0.0	3.8 $\pm$ 1.0 <sup>d</sup>
116	1.45 $\pm$ 0.24	3.17 $\pm$ 0.29 <sup>d</sup>	0.0 $\pm$ 0.0	5.2 $\pm$ 0.2 <sup>d</sup>

<sup>a</sup> Values represent means  $\pm$  SE ( $N=6$ ).

<sup>b</sup> Values represent means  $\pm$  SE ( $N=5$ ).

<sup>c</sup> Values are the sum of the scores for lesion severity and distribution.

<sup>d</sup> Indicates a significant difference ( $p < 0.05$ ) vs. corresponding control.

Note: N.D. = not determined.



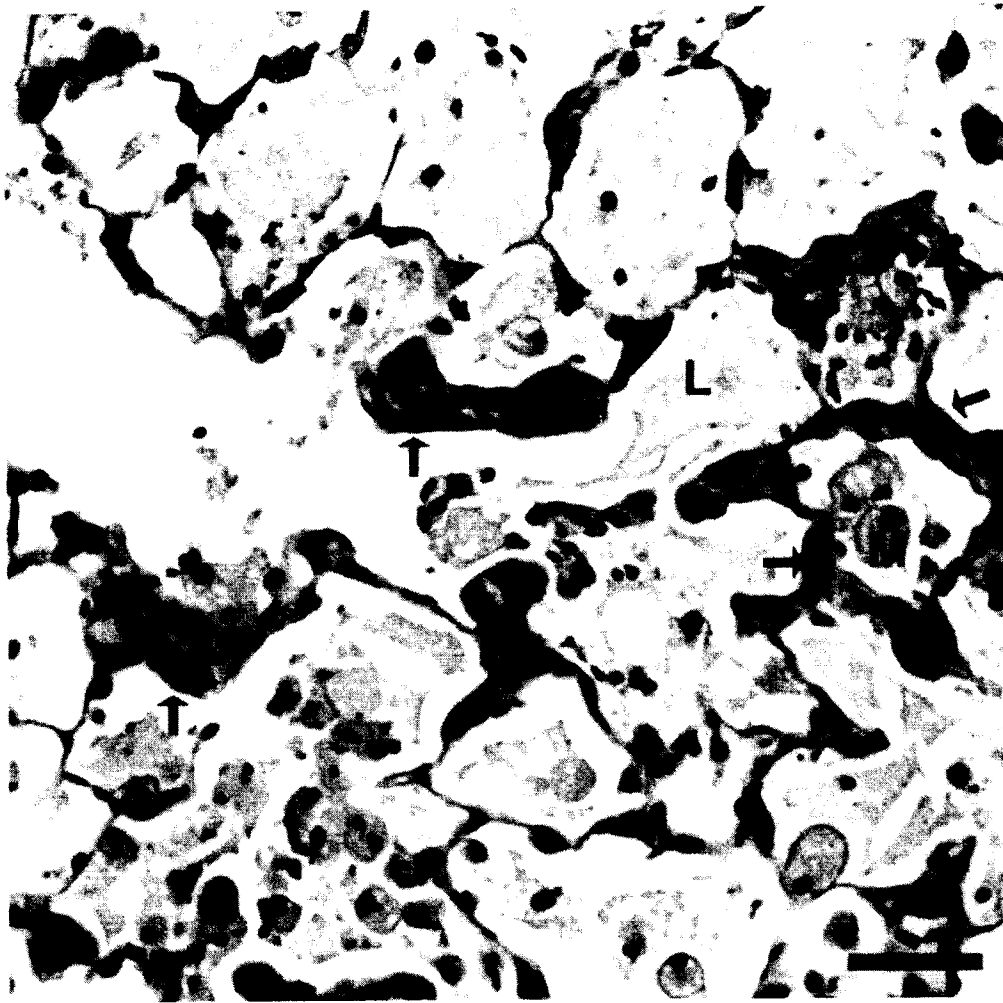


**FIGURE 8.** Photomicrograph of the lung from a rat exposed to silica for 116 days. Morphologic alterations include alveolar epithelial cell hypertrophy and hyperplasia (arrows), alveolar lipoproteinosis (L), and alveolitis with principal inflammatory cells being the alveolar macrophage (M). Scale bar = 50  $\mu$ .

minimal, histiocytic, and suppurative alveolitis and the multifocal presence of small numbers of enlarged alveolar epithelial cells, consistent with alveolar type II cell hypertrophy and hyperplasia. Both the inflammatory and epithelial responses were progressively more severe and widespread at 41 and 79 days of exposure. At 41 days of exposure, granulomatous inflammation was observed in the bronchus-associated lymphoid tissue (BALT) in three of five rats examined.

At 79 and 116 days of exposure, all rats had multifocal to multifocal and coalescent, moderate, histiocytic, and suppurative alveolitis with associated moderate, alveolar epithelial cell hypertrophy and hy-

perplasia. At 79 and 116 days of exposure, alveolar lipoproteinosis was seen in all silica-exposed rats. Granulomatous inflammation was also observed in the BALT of all rats at these time points. Fibrosis lagged behind the inflammatory response and was not observed at 41 days of exposure. However, interstitial fibrosis of alveolar septa was seen in 4 of 5 rats at 79 days of exposure. All rats had pulmonary fibrosis at 116 days of exposure, which was characterized by multifocal to multifocal and coalescent, mild, interstitial fibrosis. Alveolitis, granulomatous inflammation of the BALT, pulmonary fibrosis, and alveolar epithelial cell hypertrophy and hyperplasia were not seen in control rats.

TABLE 4. Summary of Histopathological Alterations<sup>a</sup>

Exposure day	Alveolitis <sup>b</sup>		Alveolar epithelial hypertrophy and hyperplasia <sup>b</sup>		Alveolar Lipoproteinosis <sup>b</sup>	
	Air	Silica	Air	Silica	Air	Silica
1	N.D.	0.0 ± 0.0	N.D.	0.0 ± 0.0	N.D.	0.0 ± 0.0
5	N.D.	0.0 ± 0.0	N.D.	0.0 ± 0.0	N.D.	0.0 ± 0.0
10	0.0 ± 0.0	0.0 ± 0.0	0.0 ± 0.0	0.0 ± 0.0	0.0 ± 0.0	0.0 ± 0.0
20	0.0 ± 0.0	4.0 ± 0.0 <sup>c</sup>	0.0 ± 0.0	4.0 ± 0.0 <sup>c</sup>	0.0 ± 0.0	0.0 ± 0.0
41	0.0 ± 0.0	4.8 ± 0.2 <sup>c,d</sup>	0.0 ± 0.0	5.2 ± 0.4 <sup>c,d</sup>	0.0 ± 0.0	0.0 ± 0.0
79	0.0 ± 0.0	6.6 ± 0.3 <sup>c,e</sup>	0.0 ± 0.0	6.6 ± 0.3 <sup>c,e</sup>	0.0 ± 0.0	6.2 ± 0.5 <sup>c</sup>
116	0.0 ± 0.0	7.0 ± 0.0 <sup>c,e</sup>	0.0 ± 0.0	7.0 ± 0.0 <sup>c,e</sup>	0.0 ± 0.0	8.0 ± 0.0 <sup>c,f</sup>

<sup>a</sup> Values for the histopathology scores are the sum of the severity and distribution scores.

<sup>b</sup> Values represent means ± SE (*N* = 5).

<sup>c</sup> Indicates significant difference (*p* < 0.05) vs. air-exposed control.

<sup>d</sup> For silica-exposed rats, significantly higher (*p* < 0.05) vs. 20-day exposure.

<sup>e</sup> For silica-exposed rats, significantly higher (*p* < 0.05) vs. 41-day exposure.

<sup>f</sup> For silica-exposed rats, significantly higher (*p* < 0.05) vs. 79-day exposure.

Note: N.D. = not determined.

## Discussion and Conclusions

For this study, target levels for the silica aerosol concentration and silica particle size were set at 15 mg/m<sup>3</sup> and ≤3 μm, respectively. This silica aerosol concentration was selected based on calculations that predicted sufficient silica deposition would occur to result in the development of pulmonary fibrosis in the later stages of the exposure. The silica particle size was set at ≤3 μm, because particles of this size are considered respirable in the rat.

The silica aerosol concentration was monitored by two independent methods. The first method was optical, using a RAS-2 particle sensor. Use of the RAS-2 particle sensor allowed real-time monitoring of the silica aerosol concentration. Consequently, any deviation from the target particle concentration could be immediately observed and promptly corrected. The second method used to monitor the silica aerosol concentration was gravimetric determinations made at hourly intervals throughout the study. These gravimetric determinations indicated that the silica aerosol concentration ranged from 14.9 to 15.5 mg/m<sup>3</sup> silica during the study (Table 1). Further examination of these data indicated that the silica aerosol concentration had a minimum of 8.3 mg/m<sup>3</sup> silica, median at 15.3 mg/m<sup>3</sup> silica, and max-

imum at 31.5 mg/m<sup>3</sup> silica, with 95% of the data in the 12.4–17.8 mg/m<sup>3</sup> silica range.

Another critical requirement of the silica aerosol generation system was that the silica aerosol should consist of respirable size particles. In this study, silica particle size was determined with an Anderson 8-stage cascade impactor on eight predetermined days during the study. The data indicate the silica aerosol particle size averaged ≤2 μm, and thus was in the respirable particle size range for rats.

When considered together, these data indicate that the silica aerosol generation and exposure system operated exceptionally well, providing a consistent silica aerosol concentration of 15 mg/m<sup>3</sup> of respirable size particles.

Lung silica burden was determined at various times during the exposure (Fig. 4). Oberdorster et al.<sup>21</sup> defined the initiation of lung overload as the point at which the volume of particulate in the lung is ≥10% of the lung alveolar macrophage (AM) volume. In this study, the percent of AM volume occupied by silica was estimated to be 7% after 116 days of exposure, and thus would not be considered in overload. These calculations were made using the 116-day exposure values for silica lung burden and number of AM lavaged, a silica density = 2.64 × 10<sup>3</sup> mg/mL, and a mean AM volume of 1200 μm<sup>3</sup>. Further support for this con-

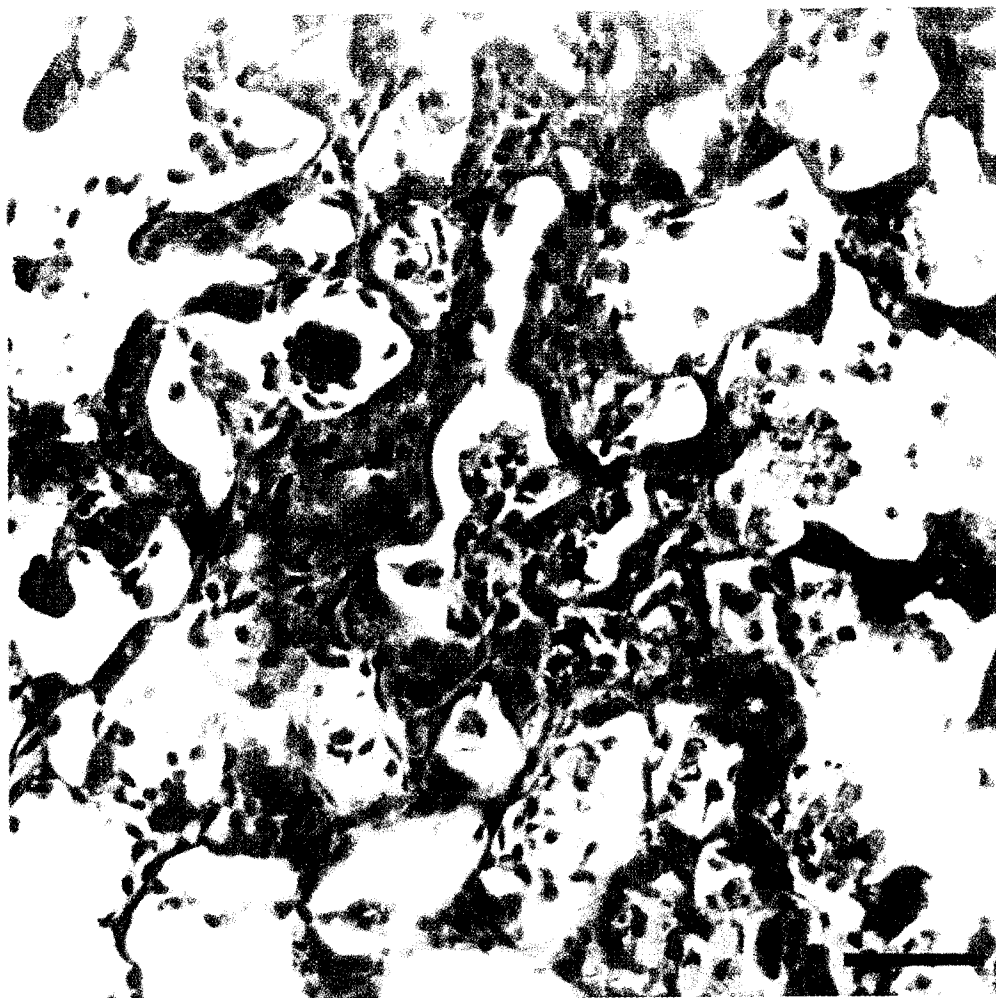


**FIGURE 7.** Photomicrograph of the lung from a rat exposed to silica for 116 days. The section is stained with Masson's trichrome, and foci of fibrosis are blue. Scale bar = 50  $\mu$ .

clusion comes from the analysis of the lung burden graph (Fig. 4), which demonstrates that no significant increase in silica lung burden had occurred from 79 to 116 days of exposure, suggesting that lung clearance and the rate of silica deposition in the lung had reached an equilibrium state. If the equilibrium state had not been reached, lung silica burden would have increased markedly.<sup>22</sup>

There is considerable debate in the field of respiratory toxicology about the role of particle overload in the development of nonneoplastic and neoplastic outcomes in rats.<sup>11</sup> Previous studies have established that lung particle overload is associated with chronic inflammation and interstitial fibrosis in rats.<sup>23</sup> However, data from this study indicate that the progres-

sive development of alveolar hypertrophy and hyperplasia, lipoproteinosis, and pulmonary fibrosis occurred despite the absence of particle overload.

Several biological and histopathological endpoints were examined during the silica exposure to evaluate the biological response to silica inhalation. On a gross level, rat body weights were monitored throughout the study as an indicator of the general health of the rats. Both air- and silica-exposed rats had similar body weights except at 79 and 116 exposure days, where the silica-exposed rat body weights were significantly higher than air-exposed controls (Fig. 2). However, this weight difference was relatively small, being 3–4% higher than control. The increase in the silica-exposed rat body weights was

partially due to increases in their lung weights. It is also possible that silica exposure decreased the physical activity, which resulted in a slight weight gain.

In contrast to the rat body weights, significant differences between the silica- and air-exposed rat lung weights were observed at 10 days of exposure (Fig. 3). At 10 days of exposure, the lung weights of silica-exposed rats were 12% higher than those of air-exposed controls, and this difference increased to 243% at 116 exposure days. This increase in the lung weight of silica-exposed rats may reflect a combination of silica deposition in the lung, recruitment of inflammatory cells into the lung, lipoproteinosis, edema, and deposition of fibrotic tissue.

A well-documented response to inhaled silica is the development of lipoproteinosis. Alveolar lipoproteinosis in silicosis is believed, at least in part, to result from enhanced production and secretion of phospholipids and surfactant proteins by alveolar Type II cells.<sup>24,25</sup> In this study, we determined BAL phospholipid levels as an index of alveolar lipoproteinosis. One might expect BAL fluid total protein concentration to increase as an indication of surfactant protein production. However, silica inhalation is also known to increase immunoglobulin levels in BAL fluid<sup>26</sup> and damage to the alveolar air/blood barrier, causing protein to leak into the alveolar spaces; thus, BAL total protein concentration reflects not only BAL surfactant protein concentrations, but other proteins indicating lung damage as well. BAL fluid isolated from silica-exposed rats had significantly higher concentrations of total protein and phospholipids beginning at 16 and 5 days of exposure, respectively (Figs. 5 and 6). Examination of the values for these BAL fluid markers in silica-exposed rats also demonstrated that they had significant progressive increases throughout the study. This progressive increase in lipoproteinosis, as indicated by BAL fluid total protein and phospholipid concentrations, is in agreement with the progression of inflammation and damage detected histologically (Table 4).

Indeed, the major histopathologic alterations seen in this study are alveolitis, alveolar type II cell hyperplasia, lipoproteinosis, and interstitial fibrosis. Similarly, the spectrum of human pulmonary responses to silica exposure includes alveolitis, alveolar type II cell hyperplasia, and interstitial fibrosis.<sup>27-31</sup>

Pulmonary fibrosis was assessed both biochemically and histologically. Hydroxyproline, an amino acid unique to collagen, was measured at various times in lung tissue isolated from air- and silica-exposed rats and indicated that fibrosis had developed at 116 days of exposure (Table 3). Fibrosis was detected at 79 days of exposure by the histological examinations, and was more severe by 116 days of exposure (Table 3).

An interesting phenomenon becomes apparent when the data on lung weight, acellular BAL total protein, phospholipid concentrations, and silica lung burden are considered together. For silica-exposed rats, from the start of the silica exposure until 41 days of exposure, the values for lung weight, acellular BAL total protein, and acellular BAL phospholipid concentrations were elevated above control but remained relatively constant. During this same period, silica lung burden steadily increased. After 41 days of exposure, lung weight, acellular BAL total protein, and acellular BAL phospholipid concentrations markedly increased, whereas the amount of silica in the lung leveled off. These observations suggest that, initially, pulmonary defense mechanisms were able to compensate and control silica-induced pulmonary damage until a rather defined point in the exposure. Thereafter, the effects of silica overwhelmed these compensatory mechanisms, and pulmonary damage increased rapidly. Interestingly, pulmonary fibrosis was first detected histologically at 79 days of exposure—that is, after the silica-induced pulmonary damage began to rapidly increase.

Several major observations were made in this study. First, characterization of silica dust in the inhalation chamber demonstrates that the silica aerosol generation and exposure system performed extremely well, providing a constant silica aerosol concentration of respirable size silica particles in an exposure chamber with good overall air quality. Second, we established the characteristics of silica deposition in the rat lung and determined that the lungs were not in overload. The progressive development of lipoproteinosis and pulmonary fibrosis occurred despite the absence of overload. Taken together, these results provide the basis to validate this silica aerosol generation and exposure system for use in subsequent investigations of the mechanisms of silica-induced pulmonary fibrosis.

## References

1. Banks DE. Clinical features of silicosis. In: Castranova V, Vallyathan V, Wallace WE, editors. *Silica and silica-induced lung diseases*. Boca Raton FL: CRC Press; 1996.
2. Sanderson WT. The U.S. population-at-risk to occupational respiratory diseases. In: Merchant JA, editor. *Occupational respiratory diseases*. Washington, DC: DHHS (NIOSH) publication 86-102; 1986.
3. Graham WG. Silicosis. *Clin Chest Med* 1992;13: 253-267.
4. Friedetzky A, Garn H, Kirchner A, Gemsa D. Histopathological changes in enlarged thoracic lymph nodes during the development of silicosis in rats. *Immunobiology* 1998;199:119-132.
5. Mohr C, Davis GS, Graebner C, Hemenway DR, Gemsa D. Enhanced release of prostaglandin E2 from macrophages of rats with silicosis. *Am J Respir Cell Mol Biol* 1992;6:390-396.
6. Driscoll KE, Lindenschmidt RC, Maurer JK, Perkins L, Perkins M, Higgins J. Pulmonary response to inhaled silica or titanium dioxide. *Toxicol Appl Pharmacol* 1991;111:201-210.
7. Henderson RF, Driscoll KE, Harkema JR, Lindenschmidt RC, Chang IY, Maples KR, Barr EB. A comparison of the inflammatory response of the lung to inhaled versus instilled particles in F344 rats. *Fund Appl Toxicol* 1995;24:183-197.
8. Johnston CJ, Driscoll KE, Finkelstein JN, Baggs R, O'Reilly MA, Carter J, Gelein R, Oberdorster G. Pulmonary chemokine and mutagenic responses in rats after subchronic inhalation of amorphous and crystalline silica. *Toxicol Sci* 2000;56:405-413.
9. Dey RD, Stanley C, Blackford JA Jr, Harness J, Durham J, Castranova V, Hubbs A. Inhaled silica dust increases nitric oxide and cytokine production associated with collagen synthesis and fibrosis in rats. *Appl Occup Environ Hyg* 1996;11:914-918.
10. Muhle H, Bellmann B, Creutzenberg O, Dasenbrock C, Ernst H, Kilpper R, MacKenzie JC, Morrow P, Mohr U, Takenaka S, Mermelstein R. Pulmonary response to toner upon chronic inhalation exposure in rats. *Fund Appl Toxicol* 1991;17:280-299.
11. ILSI Risk Science Institute Workshop Participants. The relevance of the rat lung response to particle overload for human risk assessment: a workshop consensus report. *Inhal Toxicol* 2000;12:1-17.
12. NTP. Specifications for the conduct of studies to evaluate the toxic and carcinogenic potential of chemical, biological and physical agents in laboratory animals for the National Toxicology Program. Research Triangle Park NC: National Toxicology Program, 1992.
13. Bartlett GR. Phosphorus assay in column chromatography. *J Biol Chem* 1958;234:466-468.
14. Oyarzun MJ, Clements JA. Control of lung surfactant by ventilation, adrenergic mediators, and prostaglandins in the rabbit. *Am Rev Respir Dis* 1978; 117:879-891.
15. Kivirikko KI, Laitinen O, Prockop DJ. Modifications of a specific assay for hydroxyproline in urine. *Anal Biochem* 1967;19:249-255.
16. Ma JY, Barger MW, Hubbs AF, Castranova V, Weber SL, Ma JK. Use of tetrandrine to differentiate between mechanisms involved in silica- versus bleomycin-induced fibrosis. *J Toxicol Environ Health* 1999;57: 247-266.
17. Hubbs AF, Castranova V, Ma JYC, Frazer DG, Siegel PD, Ducatman BS, Grote A, Schwegler-Berry D, Robinson VA, Van Dyke C, Barger M, Xiang J, Parker J. Acute lung injury induced by a commercial leather conditioner. *Toxicol Appl Pharmacol* 1997; 143:37-46.
18. Searle SR. *The 2-way crossed classification. Linear models*. New York: Wiley; 1971.
19. Hollander M, Wolfe DA. *The two-sample location problem. Nonparametric statistical methods*. New York: Wiley; 1973.
20. Myers RH. *The multiple linear regression model. Classical and modern regression with applications*. Boston: PWS-Kent; 1990.
21. Oberdorster G, Ferin J, Morrow PE. Volumetric loading of alveolar macrophages (AM): a possible basis for diminished AM-mediated particle clearance. *Exp Lung Res* 1992;18:87-104.
22. Miller FJ. Dosimetry of particles in laboratory animals and humans in relationship to issues surrounding lung overload and human health risk assessment: a critical review. *Inhal Toxicol* 2000;12: 19-57.
23. Donaldson K. Nonneoplastic lung responses induced in experimental animals by exposure to poorly soluble nonfibrous particles. *Inhal Toxicol* 1999;12: 121-139.
24. Crouch E, Persson A, Chang D, Parghi D. Surfactant protein D. Increased accumulation in silica-induced pulmonary lipoproteinosis. *Am J Pathol* 1991; 139:765-776.
25. Hook GE. Alveolar proteinosis and phospholipidosis of the lungs. *Toxicol Pathol* 1991;19: 482-513.
26. Huang SH, Hubbs AF, Stanley CF, Vallyathan V, Schnabel PC, Rojanasakul Y, Ma JK, Banks

- DE, Weissman DN. Immunoglobulin responses to experimental silicosis. *Toxicol Sci* 2001;59:108–117.
27. Craighead JE, Abraham JL, Churg A, Green FH, Kleinerman J, Pratt PC, Seemayer TA, Vallyathan V, Weill H. The pathology of asbestos-associated diseases of the lungs and pleural cavities: diagnostic criteria and proposed grading schema. Report of the Pneumoconiosis Committee of the College of American Pathologists and the National Institute for Occupational Safety and Health. *Arch Pathol Lab Med* 1982;106:544–596.
28. Rom WN. Relationship of inflammatory cell cytokines to disease severity in individuals with occupational inorganic dust exposure. *Am J Ind Med* 1991;19:15–27.
29. Seaton A, Legge JS, Henderson J, Kerr KM. Accelerated silicosis in Scottish stonemasons. *Lancet* 1991;337:341–344.
30. Honma K, Chiyotani K. Pulmonary alveolar proteinosis as a component of massive fibrosis in cases of chronic pneumoconiosis. An autopsy study of 79 cases [see comments]. *Zentralblatt für Pathologie* 1991;137:414–417.
31. Green FHY, Vallyathan V. Pathological responses to inhaled silica. In: Castranova V, Vallyathan V, Wallace WE, editors. *Silica and silica-induced lung diseases*. Boca Raton FL: CRC Press; 1996.